Nucleus-nucleus scattering in the perturbative QCD

M.A.Braun[a*]

[a] *Dep. High-Energy physics, S.Petersburg University*
198504 S.Petersburg, Russia

Abstract

Nucleus-nucleus interaction is studied in the framework of the perturbative QCD with $N_c \to \infty$ and a fixed coupling constant. The pomeron tree diagrams are summed by an effective field theory. The classical field eqations are solved by iteration procedure, which is found convergent in a restricted domain of not too high energies and atomic nucmbers. The found gluon distributions do not scale, have their maxima close to 2 GeV independent of rapidity and fall towards the central rapidity region. The cross-sections slowly grow with energy due to the contributiom from peripheral collisions, where evolution remains linear. Simple variational extimates at higer rapidities confirm this tendency. Inclusive cross-section for gluon jet production are calculated

1 Introduction

The study of high-energy scattering in the framework of the perturbative QCD in the Regge kinematics, in which the $s >> t >> \Lambda^2$, began with the work of M.T.Grisaru *et al.* [1] in which it was shown that in the gluon t-channel the amplitude is described by a contribution of a Regge pole with the gluon quantum number and intercept equal to unity. Thus the gluon reggeizes in the QCD, which is an intrinsic property of non-abelian gauge theories. The next decisive step was made in the seminal papers [2] where the vacuum channel was studied and it was shown that it is described by the exchange of a colorless object consisting of two reggeized gluons with the intercept $\Delta(0)$ higher than unity: the BFKL, or hard, pomeron. In fact the BFKL pomeron is not a Regge pole, but rather a Regge cut starting from $\Delta(0)$ at $t = 0$. From the start it was clear that the BFKL pomeron is not free from problems. The most fundamental of them is that its derivation is made within the fixed coupling constant approximation. This problem has not been solved up to the present. In fact that it is closely related to the confinement problem, since in the BFKL kinematics transverse momenta are not restricted from below. A more tractable problem is that even if in the initial state the transverse momenta are high, so that perturbative treatment is reliable, the system gradually evolves to include smaller and smaller momenta: diffusion into infrared. This problem can be avoided if the initial momenta are sufficiently high and evolution is restricted to not too large energies. Finally the cross-section described by the BFKL pomeron grows as a power of energy in contradiction with the Froissart theorem and as a result multiple pomeron exchange starts to dominate at high rapidities.

This latter circumstance received considerable attention in the last decades. Pioneered by the work of J.Bartels [3] exchange of more than two reggeized gluons has been studied. A vertex for splitting a pair of reggeized gluons into four has been found. As a simplifying tool the high-colour limit of the QCD was studied with special emphasis. A very efficient colour dipole formalism has been proposed by A. Mueller *et al.* [4] and N.Nikolaev and B.G.Zakharov [5] in this approach. It was demonstrated that in the high-colour limit the high-energy amplitude can be described by the exchange of BFKL pomerons with a triple pomeron interaction [6].

*e-mail: braun1@pobox.spbu.ru

An equation which sums all pomeron fan diagrams was presented in [7, 8] and first solved numerically in [9]. In the last paper it was demonstrated that the characteristic momenta involved in the fans grow with energy, so that the problem of diffusion into infrared is eliminated.

For nucleus-nucleus scattering the situation complicates enormously. The basic complication comes from the fact that now the pomerons not only split into two but also merge from two to one. The dominating tree diagrams now do not reduce to fans but involve more complicated structures. Still as we shall see, using methods of the effective non-local field theory, one can sum all these diagrams, reducing the problem to the solution of a pair of non-linear field equations in the rapidity-transverse-momentum space [10]. Unfortunaltely, contrary to the non-linear BFKL equation, these are not evolution equations but rather correspond to a system of full-fledged non-linear integral equations, which are very difficult to solve.

Here we desribe first attempts at a solution of these equations and try to gain some insight into the physical picture of the nucleus-nucleus interaction in this approach Our results are very preliminary and cover a restricted domain of rapidities and atomic numbers. They show that in the nucleus-nucleus collisions the rise of the effective number of gluons becomes still more suppressed than in the non-linear BFKL equation case. In fact variational estimates indicate that it may even go down with the growth of the rapidity. However this does not clearly reflect itself on the final nucleus-nucleus cross-sections, which continue to slowly rise due to the contribution from the peripheral parts of the nuclei, where, due to the small nuclear density, the evolution remains practically linear.

We also present the inclusive cross-sections for gluon jet production in nucleus-nucleus collisions. Unlike the total cross-section they do not require solving complicated equations for the nucleus-nucleus amplitude but only summing fan digrams propagating from the observed gluon jet to both projectile and target nuclei. So our results for the inclusive cross-sections are complete and reliable. They indicate that due to pomeron interaction the cross-sections are proportional to the number of participants and not to the number of interactions.

2 AB-cross-sections and effective field theory

At fixed overall impact parameter b and (high) rapidity Y the nucleus-A-nucleus-B total cross-section is given by

$$\mathcal{A}(Y,b) = 2\left(1 - e^{-T(Y,b)}\right). \tag{1}$$

Here the eikonal function T is a contribution from the connected part and is an integral over two impact parameters b_A and b_B of the collision point relative to the centers of the nuclei A and B:

$$T(Y,b) = \int d^2b_A d^2b_B \delta^2(b - b_A + b_B) T(Y, b_A, b_B). \tag{2}$$

In the perturbative QCD in the large N_c limit the amplitude $-T(Y, b_A, b_B)$ is given by a sum of all connected tree diagrams constructed of BFKL pomerons which interact between themselves via the triple pomeron vertex. It can be shown that this sum is generated by an effective field theory of two fields $\phi(y,q)$ and $\phi^\dagger(y,q)$ depending on rapidity y and transverse momentum q with an appropriately chosen action S [10]. It is convenient to rescale the rapidities introducing $\bar{y} = \bar{\alpha} y$ where standardly $\bar{\alpha} = \alpha_s N_c/\pi$. The action consists of a free part S_0, interaction part S_I and external part S_E. The free part is given by

$$S_0 = \frac{1}{2\alpha_s^2} \langle \phi^\dagger K \left(\frac{\partial}{\partial \bar{y}} + H \right) \phi \rangle, \tag{3}$$

where H is BFKL forward Hamiltonian, divided be $\bar{\alpha}$ and K is a differential operator in q commuting with H

$$K = \nabla_q^2 q^4 \nabla_q^2. \tag{4}$$

Symbol $\langle ... \rangle$ means integrating over y and q with weight $1/(2\pi)^2$. Action S_0 generates propagators which are BFKL Green function with operators K^{-1} attached at their ends. The interaction part of the action describes splitting and merging of pomerons:

$$S_I = \frac{1}{2\alpha_s^2}\langle\Big({\phi^\dagger}^2 K\phi + \phi^2 K\phi^\dagger\Big)\rangle. \tag{5}$$

Finally the external action is

$$S_E = -\frac{1}{2\alpha_s^2}\langle\phi^\dagger K\phi\Big(\delta(y) + \delta(y-Y)\Big)\rangle, \tag{6}$$

where we expressed the external sources via the given boundary values of ϕ at $y = 0$ and $\phi^\dagger$ at $y = Y$.

The classical equations of motion which follow, multiplied by $(1/2)K^{-1}$ from the left, are

$$\left(\frac{\partial}{\partial y} + H\right)\phi + \Big(\phi^2 + 2K^{-1}\phi^\dagger K\phi\Big) = 0 \tag{7}$$

and

$$\left(-\frac{\partial}{\partial y} + H\right)\phi^\dagger + \Big({\phi^\dagger}^2 + 2K^{-1}\phi K\phi^\dagger\Big) = 0, \tag{8}$$

with the boundary conditions

$$\phi(0,q) = \alpha_s K^{-1} w_A(q), \quad \phi^\dagger(Y,q) = \alpha_s K^{-1} w_B(q) \tag{9}$$

and $w_{A(B)}$ describing the interaction of the pomerons with nucleons in the target (projectile). If the colour distribution in the target is given by

$$\rho_A(r) = g^2 A T_A(b_A)\rho(r), \tag{10}$$

where $\rho(r)$ is the colour distribution in the nucleon and T_A is the target nucleus profile function, then $w_A(q)$ is the Fourier transform of $r^2\rho_A(r)$ and similarly for the projectile B.

The eikonal function $T(Y, b_A, b_B)$ is just the action S calculated with the solutions of Eqs. (7)and (8), ϕ_{cl} and $\phi^\dagger_{cl}$:

$$T(Y, b_A, b_B) = -S\{\phi_{cl}, \phi^\dagger_{cl}\}. \tag{11}$$

Using the equation of motions one can somewhat simplify the expression for S. Indeed multiplying the first equation by $2K\phi^\dagger$, the second one by $2K\phi$, integrating both over y and q and summing the results one obtains a relation

$$2S_0 + 3S_I + S_E = 0, \tag{12}$$

which is valid for the classical action, that is, calculated with the solutions of Eqs. (9) and (10). Using this relation we can exclude, say, S_0 from (12) to find

$$T(Y, b_A, b_B) = \frac{1}{2}\Big(S_I\{\phi_{cl}, \phi^\dagger_{cl}\} - S_E\{\phi_{cl}, \phi^\dagger_{cl}\}\Big). \tag{13}$$

The dependence on b_A and b_B comes from the boundary conditions (9).

3 Solution

3.1 Boundary conditions

The initial values for $\phi(y,q)$ were taken in several variants, inspired by the Golec-Biernat-Wuesthoff distribution, fitted to the proton data at comparatively low values of x [11]. Our results which follow correspond to Variant II with the same infrared behaviour but a slowlier fall of the distribution at large q

$$\phi(0,q) = -\frac{1}{2} a \ln\left(1 + \frac{0.21814}{q^2}\right). \tag{14}$$

Here a carries information about the nucleus and impact parameter

$$a = \sigma_0 T_A(b_A), \tag{15}$$

with $\sigma_0 = 20.8$ mb and q in GeV/c. The value of $\phi^\dagger(Y,q)$ was taken in the same form with $T_A(b_A) \to T_B(b_B)$.

3.2 Iterative solution

Our first method to find the minimum value of the classical action has been to solve classical equation of motion iteratively. We have chosen the sum of pure fan diagrams as a starting function for iteration. In practice this means that we first solve the equations with the non-linear term mixing ϕ and $\phi^\dagger$ put to zero. These solutions serve as an input for the iterations $\phi^{(0)}$ and $\phi^{\dagger(0)}$. Then we find next iterations from the equations

$$\left(\frac{\partial}{\partial y} + H\right)\phi^{(n+1)} + {\phi^{(n+1)}}^2 + 2K^{-1}\phi^{\dagger(n)} K \phi^{(n)} = 0 \tag{16}$$

and

$$\left(-\frac{\partial}{\partial y} + H\right)\phi^{\dagger(n+1)} + {\phi^{\dagger(n+1)}}^2 + 2K^{-1}\phi^{(n)} K \phi^{\dagger(n)} = 0. \tag{17}$$

For each iteration we have only to evolve the initial function from $y = 0$ to $y = Y$, rather than solve the equivalent pair of two dimensional non-linear integral equations, which considerably diminishes computer time.

Unfortunately our calculations has shown that this method works only for rather small values of the participant atomic numbers and rapidity Y. The physical values of rapidities depend on the chosen value of $\bar{\alpha}$. With $\bar{\alpha} = 0.2$ for O-O collisions iterations allow to move only up to rapidities of the order 10, that is c.m. energies of the order 150 GeV/nucleon and for Pb-Pb collision the upper limit for the c.m. energy lowers to ~ 90 GeV/nucleon.

3.3 Variational solution

A clear alternative is obviously to try to directly find the stationary point for the action choosing some trial fields $\phi(y,q)$ and $\phi^\dagger(y,q)$ which satisfy the boundary conditions. The difficulty of this approach is related to the fact that the action can have more than one stationary points. In our first attempt we have chosen the simplest form for the trial fields with y and q dependence factorized. Moreover for the the y dependence we chose a simple exponential one, with a variable slope Δ, so that our trial fields have the form

$$\phi(y,q) = e^{\Delta y}\phi(0,q), \quad \phi^\dagger(y,q) = e^{\Delta(Y-y)}\phi^\dagger(Y,q). \tag{18}$$

The only variational parameter Δ was chosen to give the minimal value for action S. With these trial fields the solution for Δ always exists for any values of Y and parameter a in Eq. (14)

and moreover it corresponds to the minimum of the action. The quality of this approximation can be checked at y and b where the exact solution can be found perturbatively. At $Y = 1$ and $a = 1$ the exact values of action S (without factor $1/(2\alpha_s^2)$ is -0.0370 whereas the variational value is -0.0262.. As one observes the precision is not very high. Still we hope that the variational approach might give some indication about the behaviour of the cross-section and eikonal functions at large values of Y at which we cannot obtain the exact solution.

3.4 Numerical results [12]

We first report on the iterational solution of the field equations (16) and (17), which as mentioned is convergent at not too high values of Y, A and B. We chose to study O-O scattering ($A = B = 16$), which allowed us to obtain the solution up to $Y = 2$. Presenting our results we consider first the gluonic density, which can be related to functions $L\phi = h$ and $L\phi^\dagger = h^\dagger$ where $L = q^2\nabla_q^2$. Indeed as follows from the study of the non-linear BFKL equation the gluon density of a single heavy nucleus is given by [9]

$$\frac{dxG(x,q)}{d^2bd^2q} = \frac{N_c}{2\pi^2\alpha_s}h(y,q), \quad y = \bar{\alpha}\ln\frac{1}{x}. \tag{19}$$

We conjecture that the gluon density in the nucleus-nucleus collision at rapidity y will be given by a similar formula with contributions from both nuclei. For central collisions then

$$\frac{dxG(x,q)}{d^2bd^2q} = \frac{N_c}{2\pi^2\alpha_s}\Big(h(y,q) + h^\dagger(y,q)\Big). \tag{20}$$

Note that in the considered symmetric case $\phi^\dagger(y,q) = \phi(Y-y,q$ and so $h^\dagger(y,q) = h(y,q)$

In Fig. 1 we illustrate the total gluon density in O-O collisions at $y = 2$ given by the sum $h(y,q) + h(Y-q)$ up to a factor depending on the coupling constant value. This density has its peak at the point close to 1 GeV/c practically independent of rapidity. The height of the peak is falling towards the central region. Some diffusion towards small momenta is observed. It is however much weaker than the diffusion for the pure BFKL evolution.

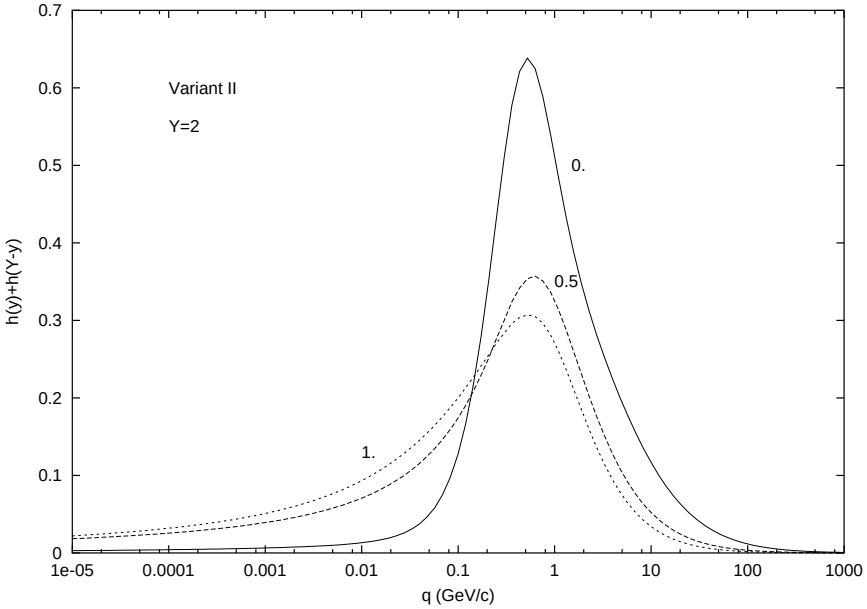

Figure 1: The total gluon density in O-O collisions. Numbers show rapidities from the target: $y = 0$, 0.5 and 2.

A clear physical observable is of course the total nucleus-nucleus cross-section obtained by the integration of (1) over all impact parameters. We show it for O-O scattering at $\bar{Y} \leq 2$ in

Fig. 2. To compare we present also the cross-sections corresponding to a single BFKL exchange. These latter are naturally larger but the difference is not at all dramatic, reaching some 5% at the maximal rapidity $\bar{Y} = 2$. This is understandable, having in mind that Eq. (1) actually automatically unitarizes the amplitude and leads to very similar results even for very different eikonal functions provided they are large. This can be clearly seen from the comparison of the eikonal functions. At $\bar{Y} = 2$ and $b = 0$ the pomeron interaction in the nucleus-nucleus collisions reduces it by a order of magnitude, although it still remains large, ~ 200. Some spreading of the gluon distribution into the low momenta domain visible in Fig. 1 in the central rapidity region makes one think that the results may be rather sensitive to the infrared region and so strongly dependent on the infrared cutoff. Such a dependence indeed exists but is not so strong. With the infrared cutoff at $k_{min} = 0.3$ GeV we obtain at $\bar{Y} = 2$ $\sigma_{O-O} = 4.18$ bn and $T_{O-O}(0) = 179$ whereas without cutoff we have $\sigma_{O-O} = 5.36$ bn and $T_{O-O}(0) = 208$. As one observes the cross-section results more sensitive to the infrared cutoff, which is a result of peripheral collisions, where evolution follows the linear BFKL equation.

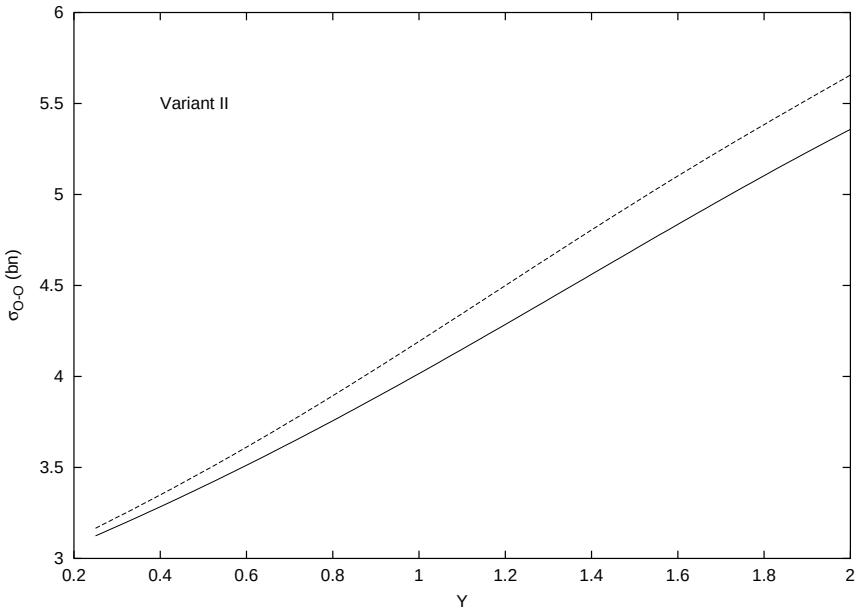

Figure 2: The total cross-section for O-O collisions. The upper curve corresponds to a single BFKL exchange

Our variational results are not restricted to small values of Y, A and B so that we followed Pb-Pb collisions ($A = B = 207$) up to $\bar{Y} = 6$, which with $\alpha_s = 0.2$ corresponds to $Y = 30$. The total cross-sections are found to steadily rise with Y. The single BFKL exchange naturally leads to larger cross-section and the ratio of these to the cross-sections with pomeronic interaction rises with Y reaching value 1.5 at $\bar{Y} = 6$. However this difference is far larger for the eikonal functions, The eikonal function for a single BFKL exchange rises up to values of the order 10^9 at $\bar{Y} = 6$, whereas with pomeronic interactions we find values around 1000. It is remarkable that, with the pomeronic interaction switched on, the eikonal actually diminishes with y for central collisions. Therefore the rise of the cross-section is totally due to peripheral collisions, where, due to low nuclear density, the non-linear effects are small and the fields grow according to the pure linear BFKL equation.

4 Inclusive gluon jet production

Emission of gluon jets in collision of two nuclei is described by a set of double fan diagrams shown in Fig. 3, which correspond to jet emission either from the connecting BFKL pomeron

or from the adjacent three-pomeron vertexes. Explicitly the inclusive cross-section $I_{AB}(y,k)$ to

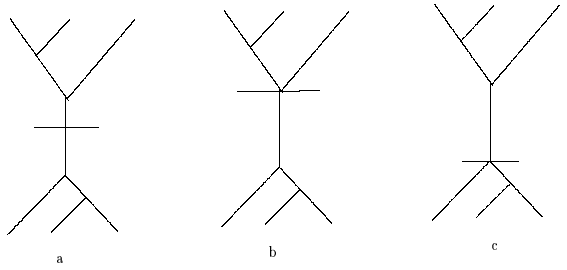

Figure 3: Typical diagrams for the inclusive cross-section in nucleus-nucleus collisions

produce a jet with the transverse momentum k at rapidity y in a collision of two nuclei with atomic numbers A and B is given by the formula

$$I_{AB}(y,k) \equiv \frac{(2\pi)^2 d\sigma}{dyd^2k} = \frac{4N_c\alpha_s}{k^2}\int d^2\beta d^2r e^{ikr}\Big[2\Delta\Phi_A(Y-y,r,\beta)\Delta\Phi_A(y,r,\beta) -$$

$$\Delta\Phi_A(Y-y,r,\beta)\Delta\Phi_A^2(y,r,\beta) -, \Delta\Phi_A^2(Y-y,r,\beta)\Delta\Phi_A(y,r,\beta)\Big]. \qquad (21)$$

where $\Phi(y,r)/r^2$ is the Fourier transform of $\phi(y,q)$ corresponding to the sum of fan diagrams only and satisfying Eq. (7) without the term mixing ϕ and $\phi^\dagger$. Solution of this equation ("BK equation") can be easily found numerically. The final cross-sections are illustrated in Figs. 4 and 5 [13]. Fig. 4 shows the momentum dependence of the cross-sections per nucleon at

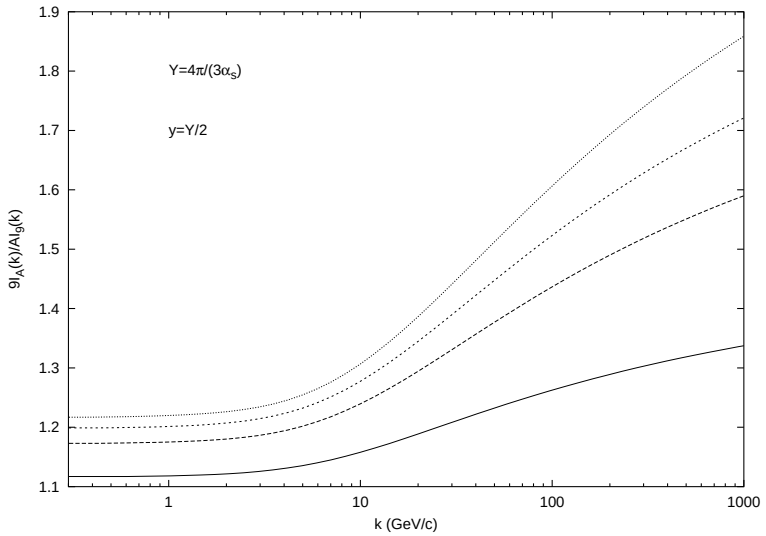

Figure 4: The ratios $(9/A)I_A(k)/I_9(k)$ for AA collisions at $\bar{Y} = 4$ and $y = Y/2$. Curves from bottom to top correspond to $A = 27, 64, 108$ and 180

midrapidity for different (identical) colliding nuclei with A = 27, 64, 108 and 180, scaled by the same quantity at $A = 9$. The collision energy corresponds to $\bar{Y} = 4$ (that is rapidity of the order 20). One observes that up to momenta of the order 10 GeV/c the cross-sections are proportional to A, that is to the number of participants, with a reasonable accuracy. At higher momenta the A dependence becomes somewhat stronger, $\sim A^{1.1}$ but it certainly does not reach the rate of growth proportional to the number of collisions ($\sim A^{4/3}$). At high momenta the

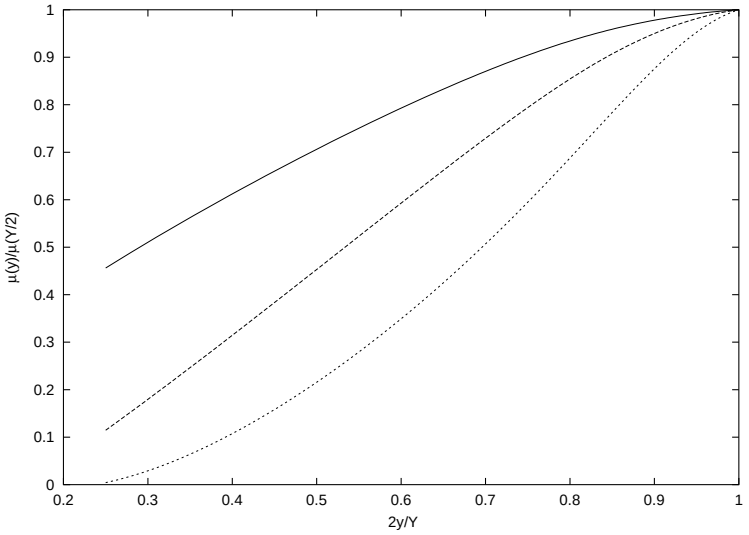

Figure 5: The form of AA multiplicities at different energies for $A = 180$. Curves from top to bottom correspond to $\bar{Y} = 2, 4$ and 8.

behaviour of the cross-sections is found to depend on energy: $I_{AA}(Y, y = Y/2, k) \sim 1/k^{p(y)}$ with $p \simeq 3.3$, 3.0 and 2.7 for $\bar{y}$=2, 4 and 8 respectively.

In Fig.5 we illustrate the change of the form of the y-dependence of the cross-section with the growth of the overall energy. We plot the ratios of multiplicities $\mu(y)$ to the multiplicity at midrapidity $\mu(Y/2)$ for $\bar{Y} = 2$, 4, and 8 for $A = 180$. One observes that the midrapidity peak becomes narrower with the growth of energy.

5 Conclusions

1. Closed equations are constructed for nucleus-nucleus scattering, which are symmetric in the projectile and target and include both splitting and fusing pomerons.

2. Up to now their exact numerical solution has been only found by iterations in the restricted domain of energies and atomic numbers.

3. The found gluon density is not scale invariant and its maximum does not seem to move towards higher momenta. The AA cross-sections grow due to their peripheric parts.

4. The inclusive cross-sections are found to be roughly proportional to the number of participants. They behave non-perturbatively in the studied region of high momenta and energies.

5. It is important to know what happens beyond the threshold of convergence of the iterative solution.

References

[1] M.T.Grisaru, H.J.Schnitzer and H.S.Tsao, Phys. Rev. **D 8** (1973) 4498.

[2] E.A.Kuraev, L.N.Lipatov and V.S.Fadin, Sov. Phys. JETP **45** (1977) 199; Ya.Ya.Balitsky and L.N.Lipatov, Sov. J.Nucl.Phys. **28** (1978) 22.

[3] J.Bartels, Nucl. Phys. **B 151** (1979) 293; **B 175** (1980) 365.

[4] A.H.Mueller, Nucl. Phys. **B 415** (1994) 373; A.H.Mueller and B.Patel, Nucl. Phys. **B 425** (1994) 471.

[5] N.N.Nikolaev and B.G. Zakharov, Phys. Lett **B 327**(1994) 15.

[6] M.A.Braun and G.P.Vacca, Eur. Phys. J. **C 6** (1999) 147.

[7] I.I.Balitsky, Nucl. Phys. **B 463** (1996) 99.

[8] Yu.V.Kovchegov, Phys. Rev. **D 60** (1999) 034008; **D61** (2000) 074018.

[9] M.A.Braun, Eur. Phys. J **C 16** (2000) 337.

[10] M.A.Braun, Phys. Lett. **B 483** (2000) 115.

[11] K.Golec-Biernat and M.Wuesthoff, Phys. Rev. **D 59** (1999) 014017; **D 60** (1999) 114023.

[12] M.A.Braun, Eur. Phys. J. **C 33** (2004) 113.

[13] M.A.Braun, Eur. Phys. J. **C 39** (2005) 451.